Agricultural and Forest Meteorology 249 (2018) 479–487

Contents lists available at ScienceDirect

Agricultural and Forest Meteorology

journal homepage: www.elsevier.com/locate/agrformet

Linking annual tree growth with eddy-flux measures of net ecosystem productivity across twenty years of observation in a mixed conifer forest

Aaron Teets[a,*], Shawn Fraver[a], David Y. Hollinger[b], Aaron R. Weiskittel[a], Robert S. Seymour[a], Andrew D. Richardson[c]

[a] School of Forest Resources, University of Maine, 5755 Nutting Hall, Orono, ME 04469, USA
[b] USDA Forest Service, Northern Research Station, 271 Mast Road, Durham, NH 03824, USA
[c] Department of Organismic and Evolutionary Biology, Harvard University, Cambridge, MA 02138, USA

ARTICLE INFO

Keywords:
AmeriFlux
Biomass increment
Howland forest
Dendrochronology
Eddy covariance
Forest carbon cycle

ABSTRACT

Eddy covariance methodologies have greatly improved our understanding of the forest carbon cycle, including controls over year-to-year variability in productivity (measured as net ecosystem productivity, NEP, where NEP is the difference between the mass of carbon fixed by photosynthesis and that lost by ecosystem respiration). However, establishing and maintaining eddy covariance towers requires sizeable financial and logistical investments. Tree-ring methods, which can produce annual estimates of tree biomass increment from individual trees, provide an alternative approach for assessing forest productivity. Attempts to link these measures of productivity (i.e., NEP and tree biomass increment) have produced inconsistent results, in part because NEP time series are typically too short to provide robust comparisons. We here use a relatively long (20-year) NEP time series together with annual tree biomass increment (derived from tree-ring data) from the same site to determine to what extent the two productivity measures relate to each other. We conducted this study at the Howland Research Forest, central Maine USA, which supports a mature, mixed-species conifer forest. We expressed stand-level tree biomass increment on a per-area basis, which allowed direct comparisons with NEP data. Our results revealed a strong relationship between tree biomass increment and annual NEP measurements when the latter are summarized from previous-year fall to current-year fall, a marked improvement over more typical calendar-year summaries. Further, our results suggest tree biomass increment lagged one year behind NEP (i.e., assimilated carbon was not allocated to wood formation until the following year) for roughly the first half of the time-series, but later became synchronized with current-year NEP. This shift to synchrony may reflect a change in stand-level carbon allocation and growth dynamics. The apparent shift in carbon allocation from storage into current-year wood formation is most evident in two recent years with above-average spring temperatures. Although our results demonstrate a link between annual tree biomass increment and NEP, they also point to complexities that may confound our interpretation of these productivity measures.

1. Introduction

Forests play a critical role in the global carbon cycle. Although details of the carbon cycle have long interested ecosystem ecologists, this interest has recently grown to include a wide range of researchers, forest managers, and policy makers as the link between atmospheric carbon dioxide (CO_2) and climate change becomes increasingly clear. Further, any efforts aimed at managing forests to partially mitigate elevated atmospheric CO_2 require a thorough understanding of the forest carbon cycle. Particularly important in our understanding of the forest carbon cycle is the inherent year-to-year variability in carbon sequestration. At the level of forest stands, annual carbon sequestration is inferred primarily from tree growth (i.e., carbon assimilated to woody tissue) or from eddy covariance (i.e., CO_2 exchange between forest canopies and the atmosphere) measurements.

Tree growth is regularly monitored for ecological studies using repeated diameter measurements of sample trees, from which net primary productivity can be inferred (Clark et al., 2001). Changes in tree biomass estimated from repeated measurements can be used to calculate the mass of carbon fixed into plant tissue. However, repeated tree measurements on an annual basis are time intensive, costly, and prone to measurement error. An alternative to repeated measurements in temperate and boreal systems is utilizing annual tree-ring records (derived from increment cores) to reconstruct previous tree diameters.

* Corresponding author at: School of Forest Resources, University of Maine, 5755 Nutting Hall, Orono, ME 04469, USA.
E-mail address: aaron.teets@maine.edu (A. Teets).

http://dx.doi.org/10.1016/j.agrformet.2017.08.007
Received 27 February 2017; Received in revised form 1 July 2017; Accepted 6 August 2017
Available online 18 August 2017
0168-1923/

Annual diameter growth can then be converted to tree biomass growth (and hence carbon gain) using published allometric equations. This method has the potential to track annual stand-level forest productivity back decades, and more importantly does not require repeated field inventories (Dye et al., 2016).

Stand-level forest productivity can also be estimated using the eddy covariance (flux) technique (Baldocchi et al., 1988). Flux towers reaching above tree canopies continuously measure net CO_2 exchange at the canopy-atmosphere interface, with a footprint (i.e., flux measurement zone) ranging from hundreds of meters to several kilometers (Baldocchi 2003). These exchanges provide robust datasets capable of inferring year-to-year variability in net ecosystem productivity (NEP). As these datasets become more temporally robust, they can be used to track whole-forest response to climate variability (Hollinger et al., 2004; Wharton and Falk 2016) and disturbance (Ueyama et al., 2011; Hicke et al., 2012), and to improve ecosystem carbon dynamics models (Richardson et al., 2010). However, establishing and maintaining eddy flux towers requires sizeable financial and logistical investments.

Tree biomass increment expressed at the stand-level can potentially serve as a proxy for NEP (measured from eddy covariance); however, the two measures differ in magnitude because they provide information on different components of the ecosystem. NEP captures the cumulative, total difference between all CO_2 sources and sinks within the entire system. While trees are the largest sink contributing to NEP in forested systems, they do not necessarily represent the annual variability in carbon exchange from other components (e.g., saplings, understory vegetation) nor carbon lost from respiration. As a result, tree biomass increment represents a subset of the carbon sink registered by NEP.

Naturally, we are led to ask to what extent the two methods for assessing productivity − tree biomass from tree-ring methods and NEP from eddy flux measures − are linked on annual timescales. If they track each other reliably, then tree-ring records could be calibrated to provide inferences about NEP for sites without flux towers. Eddy flux coupled with tree growth has been used to validate photosynthesis and transpiration rates (Catovsky et al., 2002) and to evaluate forest productivity response to climate (Grant et al., 2009; Wharton and Falk 2016). However, previous attempts to link annual NEP with tree diameter growth (Rocha et al., 2006; Zweifel et al., 2010) and tree biomass increment (Babst et al., 2013; Delpierre et al., 2016) have produced inconsistent results. For example, Babst et al. (2013) demonstrate positive correlations between tree biomass increment and early season flux measurements (January-July), yet Delpierre et al. (2016) suggest the two metrics are uncorrelated on an annual basis. These studies have been limited in part because of relatively short eddy-flux time series.

Discrepancies between tree biomass increment and NEP measurements may be due to temporary non-structural carbohydrate storage (Gough et al., 2009; Babst et al., 2013; Delpierre et al., 2016). Plants accumulate non-structural carbohydrates (primarily sugars and starch) via photosynthesis that can be mobilized and used for later growth or other plant functions (Chapin et al., 1990). Non-structural carbohydrates are critical for dormant season respiration and maintenance, and unused carbohydrates will often contribute to early season structural growth in the following year (Keel et al., 2006; Eglin et al., 2010; Michelot et al., 2011). Non-structural carbohydrate stores can last for several years; in some species they can remain in stemwood for over a decade (Richardson et al., 2013). As a result of carbohydrate storage, multi-year metrics of tree biomass increment, when compared to single-year tree biomass increment, appear to be more strongly correlated with NEP measurements (Barford et al., 2001; Curtis et al., 2002; Gough et al., 2008).

Our specific objective here was to characterize the relationship between annual tree biomass increment (from tree ring series) and annual NEP (from eddy covariance measurements). We conducted this work at the Howland Research Forest, a mature, mixed-species, multi-aged coniferous forest located in central Maine, USA. Howland has one of the longest available eddy flux time series in the USA, extending back to 1996. This long time series allowed us to not only characterize the relationship between the two methods, but also to isolate potential lag-periods of tree growth and evaluate carbon allocation strategies, improving our understanding of the forest carbon cycle. Our work builds upon previous work by Babst et al. (2013) by examining the relationship in a more complex system and over a longer time period. Our study provides a framework for tracking annual forest carbon sequestration using tree-ring methods that can be used in future studies.

2. Methods

2.1. Site description

This study was conducted in the Howland Research Forest in central Maine, USA, which is widely recognized for its long-term research in forest ecosystem science (see Rustad and Fernandez 1998; Hollinger et al., 1999; Davidson et al., 2002; Richardson et al., 2009). The site has the second longest running flux record in the US, extending back to 1996 (the longest belonging to Harvard Forest). The 20 years of data used here provide a time series long enough for robust analyses of relationships between NEP and tree biomass increment.

The Howland Forest supports a mature multi-aged forest dominated by red spruce (*Picea rubens*) and eastern hemlock (*Tsuga canadensis*), consisting of approximately 90% conifer, and 10% deciduous tree species (Table 1). Soils are spodosols, formed in well- to poorly-drained glacial till with very little elevational change. The climate is damp and cool, with average annual temperatures of 6.2 °C and a mean annual precipitation of 1148 mm (Daly et al., 2008). The site has evidence of previous logging (evenly distributed, well-decayed cut stumps) but has been unmanaged for roughly a century. Compared to other stands of the region, Howland Forest is diverse in both tree size and age distribution. The site supports several remnant trees in excess of 200 years old, along with many standing dead trees, and pit-and-mound topography.

A 3-ha permanent plot (150 × 200 m) whose center lies 240 m north of the main tower, was established in 1989 by the Laboratory for Terrestrial Physics at NASA's Goddard Space Flight Center for remote sensing and ecosystem dynamics research (see Weishampel et al., 1994; Ranson et al., 2001; Sun et al., 2011). At that time, all living and dead plot trees ≥3.0 cm diameter at breast height (DBH, 1.37 m) were mapped and measured (diameter and total height), recording ca. 7800 stems. Each tree was uniquely tagged for later re-measurement. This plot is subsequently referred to as the NASA plot. The tree species composition of the NASA plot − based on relative densities and relative basal areas (Table 1) − is nearly identical to that of the 46 continuous

Table 1
Forest descriptors by tree species in the Howland Forest NASA plot (2015 inventory). Species ranked by decreasing relative density based on trees ≥10 cm. (DBH = diameter at breast height; density refers to the number of trees per unit area.).

Species	Relativ edensity	Relative basal area	DBH (cm)		
			Mean	Std. dev.	Max.
Red spruce (*Picea rubens*)	0.447	0.413	20.1	7.1	45.2
Eastern hemlock (*Tsuga canadensis*)	0.278	0.276	20.5	8.1	50.1
N. white-cedar (*Thuja occidentalis)*	0.108	0.086	18.8	6.4	40.9
Red maple (*Acer rubrum*)	0.090	0.069	18.2	6.7	41.3
White pine (*Pinus strobus*)	0.049	0.140	33.3	17.2	68.5
Balsam fir (*Abies balsamea*)	0.021	0.006	11.7	1.5	16.9
Yellow birch (*Betula alleghaniensis*)	0.004	0.007	25.8	12.5	56.3
Paper birch (*Betula papyrifera*)	0.003	0.003	19.0	7.5	31.5

forest inventory plots established to characterize the tower footprint (Hollinger et al., 2004). These plots (each 7.3 m radius) are arrayed in concentric circles forming a 400-m radius centered on the tower. The importance values (i.e., mean of relative density and relative basal area) for the five top ranked species were strikingly similar between these two data sets: *P. rubens* = 0.43 and 0.42, *T. canadensis* = 0.28 and 0.28, *T. occidentalis* = 0.10 and 0.11, *A. rubrum* = 0.08 and 0.12, and *P. strobus* = 0.09 and 0.05, NASA plot and tower plots, respectively. Subsetting the tower plot data into smaller footprints or windward-only footprints yielded very similar results. Further, the mean diameters within species did not differ between the NASA and tower plots (t tests, all *P* values much greater than 0.05).

2.2. Forest re-inventory

In 2015, we re-located and re-measured diameters for all living and dead standing trees ≥10 cm DBH in the NASA plot. Previous species assignments and mapped locations were confirmed or corrected as necessary. Trees with equal or slightly smaller current diameters than those recorded in 1989 were assumed to have zero growth, and therefore no increase in carbon mass. These mapped datasets from 1989 and 2015 allowed us to track long-term mortality, ingrowth, diameter growth, and carbon pool change at the stand-level. These two inventories were used to estimate total tree carbon pool size on a per-ha basis in 1989 and 2015, accounting for tree mortality and ingrowth. These data are useful for studying long-term forest dynamics, but cannot be used to track annual variability in carbon mass change.

2.3. Tree biomass increment

Annual tree biomass increment was estimated from increment cores collected from a 10% subset of trees on the NASA plot at the end of the growing season in 2015. The subset was selected in a random stratified (by species and diameter class, using 10–20, 20–30, > 30 cm classes) manner, resulting in 327 trees. Although no spatial constraints were placed on the selection process, the large number of trees selected ensured adequate spatial distribution throughout the plot. The random subset is assumed to represent all living trees ≥10 cm DBH in the plot, ranging from understory suppressed trees to overstory dominants. One core was extracted from each tree at breast height with a standard 5.2 mm increment borer (Häglof, Långsele, Sweden). Cores were air-dried and secured to wooden mounts then sanded to a fine polish. Ring-widths were measured to the nearest 0.01 mm using a Velmex sliding stage (Velmex Inc., Bloomfield, NY, USA) with MeasureJ2X software (VoorTech Consulting, Holderness, NH, USA) and stereomicroscope. Cross-dating was performed using marker years, usually light or narrow rings, followed by statistical confirmation using COFECHA software (Holmes 1983). Numerous locally absent rings were identified and corrected in understory *Picea rubens* and *Tsuga canadensis*.

Tree ring measurements were used to back-calculate past diameters for every year since NASA plot establishment in 1989. Species-specific bark factors (Dixon and Keyser 2011) were used to estimate inside bark diameters in 2015. When possible, ring-widths were adjusted so that cumulative ring width equaled half the inside bark diameter in 2015, following justification presented by Frelich (2002). This adjustment compensates for off-center piths, but is only possible if cores include or approach the pith (< 15 mm) and are not affected by central rot. Ring-widths were sequentially subtracted from 2015 inside bark diameter to estimate each year's diameter inside bark. Bark thickness predicted from these diameters (using bark factors from Dixon and Keyser 2011) was then added back to each year's inside bark diameter for use in allometric equations.

Whole tree mass was estimated for each tree and each year from 1989 to 2015 using locally developed whole tree biomass equations (Young et al., 1980). Young's species specific equations have the benefit of estimating whole tree dry mass directly, including mass of the bole, branches, leaves, and coarse roots individually or as a whole. The whole-tree dry mass estimates produced from the allometric equations were converted to carbon mass by multiplying by species-specific carbon contents (Lamlom and Savidge 2003). We refer to the annual change in whole-tree carbon mass as tree biomass increment.

To express tree biomass increment on a per-area basis, we scaled growth from sampled trees to that of the entire NASA plot. Ring-width data from cored trees were used to estimate annual growth of the non-cored trees, assuming that the randomly-selected cored trees adequately represent the entire tree population on the NASA plot. To this end, we calculated total growth from 1989 to 2015 for each non-cored tree, and apportioned this growth to individual years based on estimated percent annual radial growth (from cored trees) for each species across the same diameter classes used for stratification (i.e., 10–20, 20–30, > 30 cm). This approach assumes trees within the same species and diameter classes grew similarly, which we believe is reasonable, given the relatively large number of cored trees (N = 327) and the stratified random manner in which they were selected. The annual biomass increment was thus estimated for every tree in the 2015 inventory period based on predicted ring-widths. Trees that died over the study period were not included because of unknown mortality dates; these trees were generally small-diameter, presumably slow-growing suppressed trees, and thus contributed little to tree biomass increment. Tree biomass (expressed in grams of carbon m^{-2}) was summed for all living trees, and the resulting time series reflects the year-to-year variability in carbon mass accumulated in tree tissue. The spatial variability was estimated by calculating tree biomass increment on the forty-eight 25 × 25 m subunits on the NASA plot and expressed as standard error.

2.4. Annual NEP

Net ecosystem productivity (NEP, defined as the difference between the mass of carbon fixed by photosynthesis and that lost by ecosystem respiration) was measured by eddy covariance at a tower height of 29 m and summarized from 1 January 1996–31 December 2015 as 30 min averages in units of micromoles CO_2 m^{-2} s^{-1}. The flux system on the main tower consisted of a SAT-211/3 K 3-axis sonic anemometer (Applied Technologies, Inc., Boulder, CO) and model LI-6262 fast response CO_2/H_2O infrared gas analyzer (LiCor Inc., Lincoln, NB). Air was ducted from the tower through 50 m of 3.2 mm high-density polyethylene tubing, regulated by mass flow controller at a rate of 4 L min^{-1}. The model LI-6262 analyzer was replaced with a LiCor model LI-7200 closed path analyzer in 2012. Tube length and flow rate remained unchanged. Detailed Howland flux procedures, including gap-filling and quality control can be found in Hollinger et al. (1999, 2004).

Flux data were first converted to half-hourly mean grams of carbon per square meter (g C m^{-2} s^{-1}) and then summed for each year since 1996 as the cumulative annual net carbon exchange (g C m^{-2} yr^{-1}). Tower based estimates of net ecosystem exchange are typically reported in negative units, as they reflect a micrometeorological sign convention where flux from the atmosphere is negative. For comparison to biomass increment in trees, we report NEP from the forest pool perspective: carbon into the forest is accumulated to positive values, while carbon loss to the atmosphere is negative (as presented in Richardson et al., 2013).

2.5. Linking tree biomass increment and annual NEP

Yearly NEP data are typically summarized by calendar year. Calendar year summaries are practical for carbon accounting purposes or comparisons between sites, but this timeframe holds little biological significance. Several studies have avoided a mid-winter split (calendar year) by beginning the flux year in the previous year's autumn (Goulden et al., 1996; Pereira et al., 2007). Thomas et al. (2009) summarized CO_2 fluxes by hyrdo-ecological year to study flux response to drought. Here we adopt a similar approach for summarizing flux;

however, we target the date at which stem growth terminates (i.e., end of growing season before leaf senescence). By incrementally shifting the date used to separate NEP years and comparing the correlation between tree biomass increment and NEP at each shift, we determined the optimal shift for comparing these two metrics (see section 3.3 below). In theory, this should roughly correspond with the date trees stop allocating carbon to radial growth.

We evaluated NEP measurements as the response variable in multiple linear regressions with tree biomass increment and various expressions of climate as explanatory variables. We recognize that this regression represents a reversal of typical cause and effect (i.e., biomass increment does not control NEP); however, structuring the analysis in this form allowed us to evaluate the strength and potential factors influencing the relationship between NEP and tree biomass increment. The set of potential climate variables included mean daily temperature and total precipitation summarized by year and season (three month intervals) from current and previous year using the interpolated PRISM gridded climate dataset (Daly et al., 2008). We screened this large set of variables to determine an appropriate subset for inclusion in regression models using the random forest (VSURF) package (Genuer et al., 2016) in R (R Core Team, 2014). The selected subset included mean spring temperature and previous summer precipitation. We evaluated candidate regression models using corrected Akaike's information criterion (AICc) scores, which allowed us to determine which model was best supported by the data (Burnham and Anderson, 1998). We then repeated these same tests separately for each of the four species with the highest average tree biomass increment.

3. Results

3.1. NASA plot re-inventory

An assessment of tree growth, mortality and ingrowth (small trees that achieved 10 cm DBH between 1989 and 2015) over the study period revealed an increase in plot-level carbon storage, resulting in an increase in whole-tree woody biomass stored in trees ≥10 cm from 73 (1989) to 108 Mg ha^{-1} (2015) (Table 2), that is, an average of 1.3 Mg ha^{-1} year^{-1}. Ingrowth (182 trees per hectare) exceeded tree mortality (171 trees per hectare) in the NASA plot. Trees in the 1989 dataset experienced 16.4% mortality over the 26-year period, predominantly in the smaller diameter classes.

3.2. Tree biomass increment

The total tree biomass increment (scaled to the entire plot, using growth data from cored trees) showed marked annual fluctuations over the sampling period, ranging from 131 to 177 g C m^{-2} (Fig. 1). The lowest tree biomass increments over this period were in years 1994 and 1995, immediately preceding flux measurements. The most productive year in terms of tree biomass was 2010.

3.3. Linking tree biomass increment and annual NEP

The tree biomass increment series derived from increment cores was not well correlated with the annual NEP series based on a January − December calendar year (r = 0.39). However, by incrementally shifting the dates used to define an NEP year, we determined the one-year period with the strongest correlation with tree biomass increment. As the yearly flux summary was incrementally shifted, the correlation improved dramatically (Fig. 2). For example, the correlation reached a maximum (achieving r = 0.70) by defining a flux year as August 23 of the previous year to August 22 of the following year. Based on this result, and constrained by the need to later use monthly climate data to explore climate-growth relationships, we chose to summarize the annual NEP data from previous September 1 to the following August 31 (r = 0.68). This annual summary of NEP allows us to better assess the year-to-year relationships with tree biomass increment (Fig. 1).

The mean (± SE) annual tree biomass increment (derived from tree-ring series) since 1996 was 152 ± 9 g C m^{-2} compared to 224 ± 49 g C m^{-2} of annual NEP. Although the two metrics of productivity correlate well, tree biomass increment accounted for only 68% of the total annual NEP measurements over the sampling period. When plotted together (Fig. 3), tree biomass increment and annual NEP demonstrate strong coherence. However, the relationship is interrupted by a striking shift that occurred ca. 2007. Prior to that shift, the tree biomass increment shows a distinct one-year lag behind the annual NEP data (Fig. 3), a pattern also recognized by Richardson et al. (2013) at this same site. However, after ca. 2007, this relationship changes, with flux and tree biomass increment becoming more synchronous.

Regression results also demonstrated a significant relationship

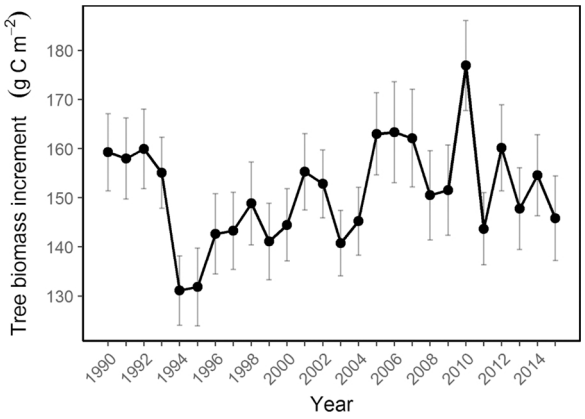

Fig. 1. Annual whole-tree biomass increment for the 3-ha NASA plot (established 1989) based on all trees ≥10 cm DBH. Error bars represent standard error calculated from forty-eight 25 × 25 m subunits of the NASA plot.

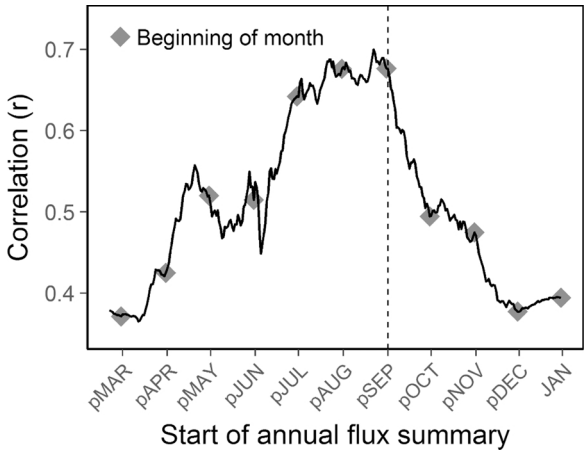

Fig. 2. The correlation with tree biomass increment when annual NEP starting dates are incrementally shifted into the previous year. The solid line represents correlation when incrementally shifted by day, and diamonds represent correlation when shifted by month. The vertical dashed line illustrates the highest monthly correlation at September 1 (r = 0.68). The prefix *p* refers to previous year.

Table 2
Forest descriptors for all trees in the NASA plot at establishment (1989) and re-measurement (2015). Whole-tree carbon mass was calculated using equations presented by Young et al. (1980).

Forest descriptors	Inventory 1989	Inventory 2015
Trees per hectare ≥10 cm	1044	1055
Basal area (m^2 ha^{-1})	29.4	40.6
Mean diameter (cm)	17.7	20.4
Total tree carbon mass (Mg ha^{-1})	73	108

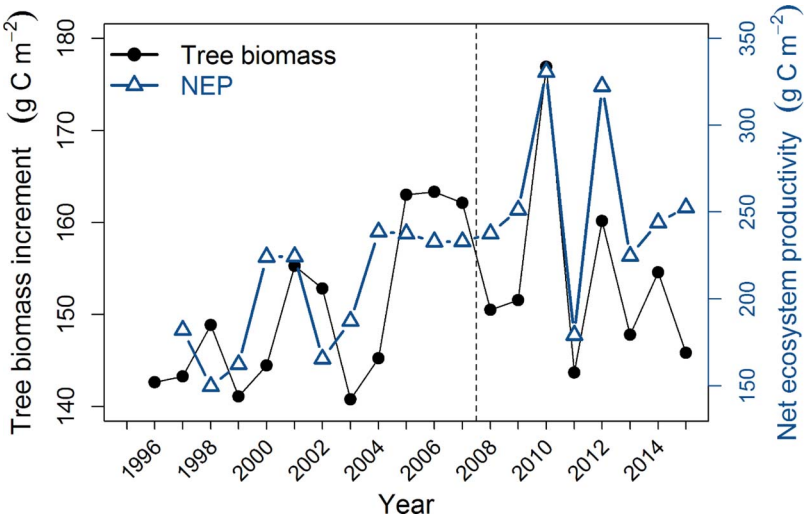

Fig. 3. Relationship between tree biomass increment (derived from tree-ring series) and annual NEP (eddy flux data), with a flux year defined as the period from previous year September 1 to following August 31 (see text). The vertical dashed line approximates the shift from a one-year lag to synchrony in the series. Error bars omitted to clarify the visual comparison of the two series.

between annual NEP and stand-level tree biomass increment. Based on the results above, we used current year tree biomass increment, one-year lagged tree biomass increment, and two climate variables (previous summer precipitation and spring temperature) as model predictors. Using biomass predictors from current and previous year, including their interaction, formed the top model (lowest AICc score), which accounted for much of the variability associated with annual NEP (R^2 = 0.67, p = 0.001, Table 3). Although the climate variables did not contribute to the top model (based on AICc scores, Table 3), we found significant positive relationships between NEP and previous summer (June-August) precipitation (p = 0.026) as well as a marginal positive relationships with spring (March-May) temperature (p = 0.056). These climate variables also demonstrated significant positive relationships with tree biomass increment (p = 0.009 and p = 0.043 respectively). When the same regression analyses were conducted separately for each species, the correlation between NEP and biomass increment seen at the stand level became much less apparent (Fig. 4). Only one species, *Tsuga canadensis*, showed a significant relationship (p = 0.001, R^2 = 0.46) between NEP and tree biomass increment (from current year, interaction not significant).

4. Discussion

This study used a 20-year NEP time series together with stand-level tree biomass increments (via tree-ring data) to determine to what extent the two productivity measures relate to each other. We demonstrated that by shifting the dates used to demarcate annual NEP summaries, we could clarify the link between tree biomass increment and annual NEP. We thus determined the optimal annual summary period (using monthly increments) to be the previous September through current August, as this summary showed the highest correlation with tree biomass increment. Starting the flux summary in September corresponds with the cessation of radial growth and the end of latewood formation of cool-weather conifers of North America (Deslauriers et al., 2003; Rossi et al., 2008; Thibeault-Martel et al., 2008; Duchesne et al., 2012), as well as increases in non-structural carbohydrate storage (Gough et al., 2009), and thus provides strong biological justification for this shift. That is, this previous September − August summary, when compared to a calendar-year summary, better represents the time period in which carbon is being allocated to a given year's tree growth. This summary period allowed us to identify a one-year lag in structural growth (relative to NEP), and it could similarly clarify relationships at other flux sites; however, the optimal period for this shift likely differs depending on tree species present and the ecosystem under study.

Table 3
Diagnostics for the top ten models (ranked by ΔAICc) for estimating NEP using stand-level tree biomass increment (TBI) from current and one-year lagged (TBI.lag) summaries, as well as climatic variables (T_spring = mean spring temperature, March-May; P_psummer = precipitation in previous summer, June-August.) Null model (intercept only) included for comparison.

Model parameters	AICc	ΔAICc	AICc Wt	R^2
TBI + TBI.lag + TBI*TBI.lag	185.3	0	0.57	0.67
TBI + TBI.lag	186.7	1.4	0.29	0.55
TBI + TBI.lag + T_spring	189.6	4.2	0.07	0.58
TBI + TBI.lag + P_psummer	190.2	4.9	0.05	0.56
TBI + TBI.lag + P_psummer + T_spring	193.9	8.6	0.01	0.59
TBI.lag + P_psummer	194.7	9.4	0.01	0.30
TBI.lag + T_spring	195.7	10.4	0	0.27
TBI	196.1	10.7	0	0.46
TBI.lag	197.1	11.8	0	0.04
TBI + T_spring	198.6	13.2	0	0.48
Null	204.8	19.5	0	–

The difference in magnitude between tree biomass increment and NEP (the latter greater than the former; Fig. 3) is partially due to unaccounted carbon sequestered in saplings, understory vegetation, and trees that died over the sampling period. Also, whole-tree allometric equations likely produce conservative estimates of primary productivity because they do not account for fine root and litter production, potentially underestimating by ca. 10–30 g C m^{-2} yr^{-1} of plant matter contributions to net soil carbon accumulation (Gaudinski et al., 2000). Additionally, uncertainties associated with landscape-level NEP may contribute to the discrepancy between measurements. For example, eddy flux measurements are sometimes biased due to inadequate measurement of nocturnal respiration (Goulden et al., 1996; Hollinger et al., 2004). Flux measurements rely on turbulence that is often suppressed at night due to atmospheric stability. A threshold is used to determine whether adequate mixing is taking place for valid measurements. A higher threshold leads to underestimating respiration, thereby overestimating NEP. These uncertainties, as well as carbon losses by mechanisms other than biological respiration (i.e., volatile or dissolved carbon compounds), may cause NEP magnitudes to differ from those of tree biomass increment. Despite the apparent difference in magnitudes, the two metrics of stand-level productivity maintain significant statistical relationships.

Our regression model suggests current and following year tree biomass increment together are useful predictors of NEP at the Howland Forest site. The significant interaction between current and following year supports our finding that tree biomass increment is lagged behind NEP over the first portion of the time series (Fig. 3), and may suggest a trade-off between current and following-year growth. Models using only one year of tree

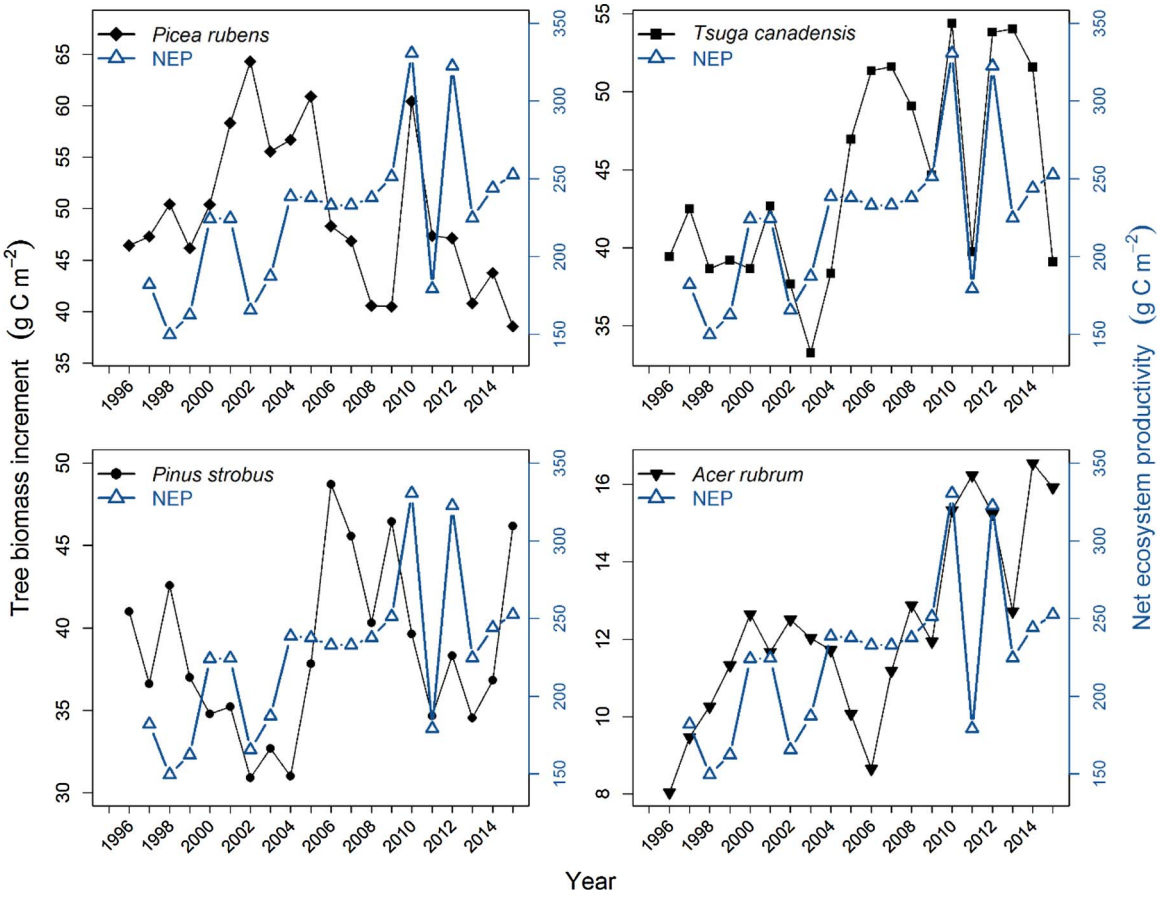

Fig. 4. Relationship between tree biomass increment (derived from tree-ring series) and annual NEP (eddy flux data) for the four tree species with the highest average tree biomass increment. Flux year defined as the period from previous year September 1 to following August 31 (see text).

biomass increment did not fit our data as well as those using two consecutive years, a finding similar to that of Barford et al. (2001) and Gough et al. (2008), who report that multi-year tree growth metrics better represent year-to-year variability in NEP. Including previous summer precipitation and spring temperature did not markedly improve our model fit, suggesting that tree biomass increment successfully captures the variability explained by these climate variables. These stand-level relationships were much less evident at the individual species level: only *Tsuga canadensis* showed a significant relationship between NEP and current-year tree biomass increment, which may indicate a higher relative contribution to NEP by this species in the tower footprint.

During the first portion of the study period, tree biomass increment shows a clear one-year lag behind annual NEP, followed by a dramatic shift to synchrony occurring ca. 2007 (Fig. 3). We interpret the early lag period as evidence that a sizeable portion of the assimilated carbon was not allocated to tree biomass growth until the following growing season, a finding also reported by Richardson et al. (2013) from this same site. Specifically, the magnitude of the previous year's flux reflected the amount of available storage that could be allocated to growth the following year.

The shift to synchrony between tree biomass increment and the annual NEP that took place ca. 2007 (Fig. 3) may reflect a period of reduced tree stress. Tree-ring records indicate years prior to the flux period (i.e., 1994 and 1995) were the lowest tree biomass increment totals in the past 26 years (Fig. 1), corresponding to below average summer precipitation in summers of 1993 and 1994 (Fig. A1), therefore suggesting some level of stress. In unfavorable conditions such as drought, stressed trees may allocate carbohydrates to storage at the expense of growth until the return of more favorable conditions (Klein et al., 2014; Hartmann et al., 2015). As a result, storage pools remain relatively stable under intermediate periods of water limitation (Deslauriers et al., 2014) or stress resulting from defoliation (Palacio et al., 2011; Wiley et al., 2013). These stored carbohydrates act as buffers against prolonged periods when carbon losses exceed gains from photosynthesis (Kozlowski, 1992). As above, previous summer precipitation demonstrated positive associations with NEP and tree biomass increment, illustrating the potential effect of water limitation on both measures of productivity. Water limitations may reduce current year photosynthesis rates, which can affect both current and following year growth (Körner 2003), or may persist over several years' growth (Anderegg et al., 2015).

The shift to synchrony is emphasized by peaks of both measurements in 2010 and 2012, both of which had early snow melt (unpublished site data) and above-average spring temperatures (Fig. A2). Favorable spring conditions can cause an earlier onset of wood formation (Rossi et al., 2008) and photosynthesis, the latter leading to increased productivity inferred from flux data (Black et al., 2000; Hollinger et al., 2004; Richardson et al., 2009). We thus speculate that increased productivity under favorable early season conditions may result in a higher proportion of current-year carbohydrates allocated to growth.

Wood formation is known to rely on a combination of current-year and previously stored non-structural carbohydrates (Kagawa et al., 2006; Keel et al., 2006). Early season growth often relies on carbohydrates stored from previous years (Kagawa et al., 2006; Gough et al., 2008; Kuptz et al., 2011), transitioning from stored to current-year sources in mid-season growth (Skomarkova et al., 2006; Kuptz et al., 2011; Carbone et al., 2013). The changing proportions of current-year versus stored carbohydrates allocated to wood formation throughout a growing season (Kuptz et al., 2011) could similarly suggest these proportions can vary from year to year depending on environmental conditions. Years with favorable early season conditions may have earlier

transitions from stored to current-year carbohydrates, and increased productivity in these years would likely result in higher proportions of current-year versus stored carbohydrates. In contrast, cooler spring temperatures (as seen in years 1994–1997; Fig. A2) may rely more heavily on previously stored carbohydrates for growth.

The trade-off between storage and growth can be explained by differences in phenology of wood formation and photosynthesis. These processes are constrained by a different set of environmental conditions (Rossi et al., 2006; Körner 2015), with wood formation being more temporally restricted than is photosynthesis on an annual basis (Körner, 2003). This phenomenon is illustrated in studies showing that annual periods of radial growth (i.e., wood formation) are significantly shorter than periods of CO_2 assimilation (Zweifel et al., 2010; Delpierre et al., 2016). Limited electronic dendrometer data from Howland Forest (Richardson, unpublished) suggest radial growth of canopy trees increases over an approximately four-month period (mid-May to mid-September). In contrast, annual NEP at Howland Forest is a net sink for approximately seven months (from 31 March until 1 November).

Unlike photosynthesis, the cessation of radial growth is less dependent on late season temperature and more dependent on photoperiod length (Rossi et al., 2008). Trees in cold climates end radial growth relatively early to ensure enough time for latewood cell wall formation and lignification before the dormant season (Rossi et al., 2008). Once radial growth terminates for a year, carbohydrates produced from September through early November (northern hemisphere) cannot be allocated to stem growth until the following season. Favorable late-season conditions would likely result in higher allocation to storage (Kuptz et al., 2011) given that stem-wood tissue is not being actively produced at this time, resulting in greater storage available for future growth. Both conifer and hardwood species accumulate non-structural carbohydrates over the growing season, reaching their annual storage maximum just before the dormant season (Gough et al., 2009; Dietze et al., 2014).

We did not expect to find the apparent shift in annual carbon allocation strategies described above. A shift from reliance on previously stored to current-year carbohydrates seems to be a reasonable explanation for the shift from a lagged to synchronous pattern of tree biomass increment (relative to NEP) documented here. These results may provide further evidence that temporary non-structural carbohydrate storage is responsible for part of the discrepancies seen between NEP and tree biomass increment (Babst et al., 2013; Gough et al., 2009). Differences in carbon allocation patterns have been documented between species (Kozlowski, 1992; Mitchelot et al., 2012; Epron et al., 2012) and throughout tree development (Genet et al., 2009). However, a shift in stand-level carbon allocation strategies, as suggested by our results, has not been previously reported.

5. Conclusions

This project assessed the relationship between annual tree biomass increment and annual NEP. Our results provide compelling evidence that the two metrics of forest productivity are related. However, yearly changes in carbon allocation strategies may alter the degree to which they are synchronized. To the best of our knowledge, a change in carbon allocation strategies has not been demonstrated at the stand level. Previous work on carbon allocation strategies has relied heavily on carbon isotope labelling, which due to the complex techniques required, is largely restricted to experiments conducted at the branch or tree level (Epron et al., 2012). Given that carbon allocation is inherently difficult to measure (Klein and Hoch, 2015), our inferences at the stand level may provide insights at a spatial scale not represented in the literature.

Climate clearly influences both metrics of forest productivity − NEP and tree biomass increment − yet each follow distinct annual cycles, likely constrained by different environmental factors. Tree biomass increment may be more challenging to link directly with climate, because a favorable year may be evident as increased growth in the following year, due to carbohydrate storage. This reasoning could in large part explain the correlation between radial growth and previous year's climate variables often reported in tree-ring studies (e.g., Fritts 1976).

In summary, we believe that stand-level tree biomass increment (derived from tree rings), as presented here, can be used as coarse proxy for interannual NEP, but should be interpreted with caution given the shift from a one-year lag to annual synchrony. Continued investigation into how these measures of productivity covary through time could provide new insights into forest carbon cycling and tree physiology.

Acknowledgements

We thank the AmeriFlux Network, USDA Forest Service Northern Research Station, and Maine Agricultural and Forest Experiment Station for providing financial support. We thank Holly Hughes, John Lee, and Bob Evans for their contributions to the continuous long-term data at the Howland Forest; Emily Anderson, Nathan Wesely, and Danae Shurn for field assistance; Mike Day and Jane Foster for insights in physiological aspects of the project; and Arun Bose for statistical guidance. Lastly, we thank the Northeastern Wilderness Trust for protecting Howland Forest.

Appendix A

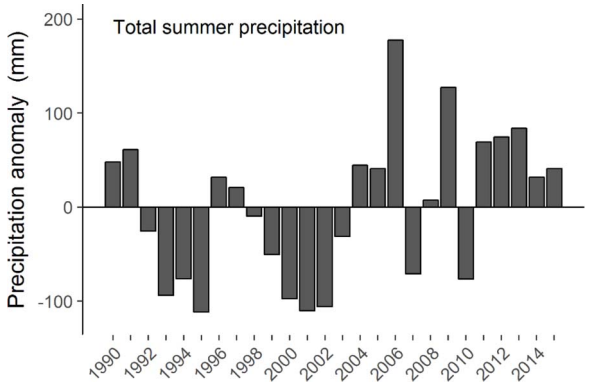

Fig. A1. Total summer precipitation anomaly summarized from June-August using the interpolated PRISM gridded climate dataset (Daly et al., 2008). The anomaly was calculated as the deviation from the average total summer precipitation from 1990 to 2015.

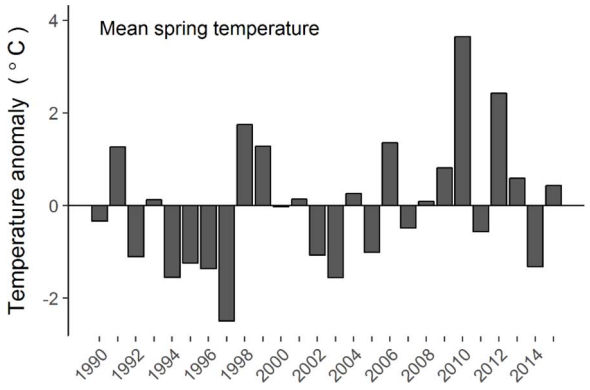

Fig. A2. Mean spring temperature anomaly summarized from May-April using the interpolated PRISM gridded climate dataset (Daly et al., 2008). The anomaly was calculated as the deviation from the average spring mean temperature from 1990 to 2015.

References

Anderegg, W.R.L., Schwalm, C., Biondi, F., Camarero, J.J., Koch, G., Litvak, M., Ogle, K., Shaw, J.D., Shevliakova, E., Williams, A.P., Wolf, A., Ziaco, E., Pacala, S., 2015. Pervasive drought legacies in forest ecosystems and their implications for carbon cycle models. Science 349, 528–532.

Babst, F., Bouriaud, O., Papale, D., Gielen, B., Janssens, I.A., Nikinmaa, E., Ibrom, A., Wu, J., Bernhofer, C., Köstner, B., Grünwald, T., Seufert, G., Ciais, P., Frank, D., 2013. Above-ground woody carbon sequestration measured from tree rings is coherent with net ecosystem productivity at five eddy-covariance sites. New Phytol. 201, 1289–1303. http://dx.doi.org/10.1111/nph.12589.

Baldocchi, D., Hinks, B., Meyers, T., 1988. Measuring biosphere-atmosphere exchanges of biologically related gases with micrometeorological methods. Ecology 69, 1331–1340.

Baldocchi, D., 2003. Assessing the eddy covariance technique for evaluating carbon dioxide exchange rates of ecosystems: past, present and future. Glob. Change Biol. 9, 479–492.

Barford, C.C., Wofsy, S.C., Goulden, M.L., Munger, J.W., Pyle, E.H., Urbanski, S.P., Hutyra, L., Saleska, S.R., Fitzjarrald, D., Moore, K., 2001. Factors controlling long- and short-term sequestration of atmospheric CO_2 in a mid-latitude forest. Science 294, 1688–1691. http://dx.doi.org/10.1126/science.1062962.

Black, T., Chen, W., Barr, A., Arian, M., Chen, Z., Nesic, Z., Hogg, E., Neumann, H., Yang, P., 2000. Increased carbon sequestration by a boreal deciduous forest in years with a warm spring. Geophys. Res. Lett. 27, 1271–1274.

Burnham, K., Anderson, D., 1998. Model Selection and Multimodel Inference. Springer Science Business Media Inc., New York, NY, USA.

Carbone, M., Keenan, T., Czimczik, C., Murakami, P., Keefe, J.O., Schaberg, P., Xu, X., Richardson, A., 2013. Age, allocation, and availability of nonstructural carbohydrates in red maple. New Phytol. 200, 1145–1155.

Catovsky, S., Holbrook, N.M., Bazzaz, F.A., 2002. Coupling whole-tree transpiration and canopy photosynthesis in coniferous and broad-leaved tree species. Can. J. For. Res. 32, 295–309. http://dx.doi.org/10.1139/x01-199.

Chapin, F.S., Schulze, E., Mooney, H.A., 1990. The ecology and economics of storage in plants. Annu. Rev. Ecol. Syst. 21, 423–447. http://dx.doi.org/10.1146/annurev.es.21.110190.002231.

Clark, D., Brown, S., Kicklighter, D.W., Chambers, J.Q., Thomlinson, J.R., Ni, J., 2001. Measuring net primary production in forests: concepts and field methods. Ecol. Appl. 11, 356–370.

Curtis, P.S., Hanson, P.J., Bolstad, P., Barford, C., Randolph, J., Schmid, H., Wilson, K.B., 2002. Biometric and eddy-covariance based estimates of annual carbon storage in five eastern North American deciduous forests. Agric. For. Meteorol. 113, 3–19. http://dx.doi.org/10.1016/S0168-1923(02)00099-0.

Daly, C., Halbleib, M., Smith, J.I., Gibson, W.P., Doggett, M.K., Taylor, G.H., Pasteris, P.P., 2008. Physiographically sensitive mapping of climatological temperature and precipitation across the conterminous United States. Int. J. Climatol. http://dx.doi.org/10.1002/joc.1688.

Davidson, E.A., Savage, K., Bolstad, P., Clark, D.a., Curtis, P.S., Ellsworth, D.S., Hanson, P.J., Law, B.E., Luo, Y., Pregitzer, K.S., Randolph, J.C., Zak, D., 2002. Belowground carbon allocation in forest estimated from litterfall and IRGA-based soil respiration measurements. Agric. For. Meteorol. 113, 39–51. http://dx.doi.org/10.1016/S0168-1923(02)00101-6.

Delpierre, N., Berveiller, D., Granda, E., Dufrêne, E., 2016. Wood phenology, not carbon input, controls the interannual variability of wood growth in a temperate oak forest. New Phytol. 210, 459–470.

Deslauriers, A., Morin, H., Begin, Y., 2003. Cellular phenology of annual ring formation of *Abies balsamea* in the Quebec boreal forest (Canada). Can. J. For. Res. 200, 190–200. http://dx.doi.org/10.1139/X02-178.

Dietze, M.C., Sala, A., Carbone, M.S., Czimczik, C.I., Mantooth, J.A., Richardson, A.D., Vargas, R., 2014. Nonstructural carbon in woody plants. Annu. Rev. Plant Biol. 65, 667–687. http://dx.doi.org/10.1146/annurev-arplant-050213-040054.

Dixon, G.E., Keyser, C.E., 2011. Northeast (NE) Variant Overview: Forest Vegetation Simulator. U.S. Department of Agriculture, Forest Service, Forest Service Management Service Center, Fort Collins.

Duchesne, L., Houle, D., Orangeville, L.D., 2012. Influence of climate on seasonal patterns of stem increment of balsam fir in a boreal forest of Québec, Canada. Agric. For. Meteorol. 162–163, 108–114. http://dx.doi.org/10.1016/j.agrformet.2012.04.016.

Dye, A., Plotkin, A.B., Bishop, D., Pederson, N., Poulter, B., Hessl, A., 2016. Comparing tree-ring and permanent plot estimates of aboveground net primary production in three eastern U.S. forests. Ecosphere 7, 1–13.

Eglin, T., Francois, C., Michelot, A., Delpierre, N., Damesin, C., 2010. Linking intra-seasonal variations in climate and tree-ring ^{13}C: A functional modelling approach. Ecol. Modell. 221, 1779–1797. http://dx.doi.org/10.1016/j.ecolmodel.2010.04.007.

Epron, D., Bahn, M., Derrien, D., Lattanzi, F.A., Pumpanen, J., Gessler, A., Högberg, P., Maillard, P., Dannoura, M., Gérant, D., Buchmann, N., 2012. Pulse-labelling trees to study carbon allocation dynamics: a review of methods, current knowledge and future prospects. Tree Physiol. 32, 776–798. http://dx.doi.org/10.1093/treephys/tps057.

Frelich, L.E., 2002. Forest Dynamics and Disturbance Regimes. Cambridge University Press, Cambridge, UK.

Fritts, H.C., 1976. Tree Rings and Climate. Academic Press, London, UK.

Gaudinski, J., Trumbore, S., Davidson, E., Zheng, S., 2000. Soil carbon cycling in a temperate forest: radiocarbon-based estimates of residence times, sequestration rates and partitioning of fluxes. Biogeochemistry 51, 33–69. http://dx.doi.org/10.1023/A:1006301010014.

Genet, H., Bréda, N., Dufrêne, E., 2009. Age-related variation in carbon allocation at tree and stand scales in beech (*Fagus sylvatica* L.) and sessile oak (*Quercus petraea* (Matt.) Liebl.) using a chronosequence approach. Tree Physiol. 30, 177–192. http://dx.doi.org/10.1093/treephys/tpp105.

Genuer, R., Poggi, J.-M., Tuleau-Malot, C., 2016. VSURF: Variable Selection Using Random Forests. R Package Version 1.0.3.

Gough, C.M., Vogel, C.S., Schmid, H.P., Su, H.-B., Curtis, P.S., 2008. Multi-year convergence of biometric and meteorological estimates of forest carbon storage. Agric. For. Meteorol. 148, 158–170. http://dx.doi.org/10.1016/j.agrformet.2007.08.004.

Gough, C.M., Flower, C.E., Vogel, C.S., Dragoni, D., Curtis, P.S., 2009. Whole-ecosystem labile carbon production in a north temperate deciduous forest. Agric. For. Meteorol. 149, 1531–1540. http://dx.doi.org/10.1016/j.agrformet.2009.04.006.

Goulden, M.L., Munger, J.W., Fan, S., Daube, B.C., Wofsy, S.C., 1996. Measurements of carbon sequestration by long-term eddy covariance: methods and critical evaluation of accuracy. Glob. Change Biol. 2, 169–182.

Grant, R.F., Barr, A.G., Black, T.A., Margolis, H.A., Dunn, A.L., Metsaranta, J., Wang, S., McCaughey, J.H., Bourque, C.A., 2009. Interannual variation in net ecosystem productivity of Canadian forests as affected by regional weather patterns − A Fluxnet-Canada synthesis. Agric. For. Meteorol. 149, 2022–2039. http://dx.doi.org/10.1016/j.agrformet.2009.07.010.

Hartmann, H., McDowell, N.G., Trumbore, S., 2015. Allocation to carbon storage pools in Norway spruce saplings under drought and low CO_2. Tree Physiol. 35, 243–252. http://dx.doi.org/10.1093/treephys/tpv019.

Hicke, J.A., Allen, C.D., Desai, A.R., Dietze, M.C., Hall, R.J., Ted Hogg, E.H., Kashian, D.M., Moore, D., Raffa, K.F., Sturrock, R.N., Vogelmann, J., 2012. Effects of biotic disturbances on forest carbon cycling in the United States and Canada. Glob. Change Biol. 18, 7–34. http://dx.doi.org/10.1111/j.1365-2486.2011.02543.x.

Hollinger, D.Y., Goltz, S.M., Davidson, E.A., Lee, J.T., Tu, K., Valentine, H.T., 1999. Seasonal patterns and environmental control of carbon dioxide and water vapour exchange in an ecotonal boreal forest. Glob. Change Biol. 5, 891–902.

Hollinger, D.Y., Aber, J., Dail, B., Davidson, E.A., Goltz, S.M., Hughes, H., Leclerc, M.Y., Lee, J.T., Richardson, A.D., Rodrigues, C., Scott, N.A., Achuatavarier, D., Walsh, J., 2004. Spatial and temporal variability in forest-atmosphere CO_2 exchange. Glob. Change Biol. 10, 1689–1706. http://dx.doi.org/10.1111/j.1365-2486.2004.00847.x.

Holmes, R.L., 1983. Computer-assisted quality control in tree-ring dating and measurements. Tree-ring Bull. 44, 69–75.

Körner, C., 2003. Carbon limitation in trees. J. Ecol. 91, 4–17.

Körner, C., 2015. Paradigm shift in plant growth control. Curr. Opin. Plant Biol. 25, 107–114. http://dx.doi.org/10.1016/j.pbi.2015.05.003.

Kagawa, A., Sugimoto, A., Maximov, T.C., 2006. $^{13}CO_2$ pulse-labelling of photoassimilates reveals carbon allocation within and between tree rings. Plant, Cell Environ. 29, 1571–1584. http://dx.doi.org/10.1111/j.1365-3040.2006.01533.x.

Keel, S.G., Siegwolf, R.T.W., Körner, C., 2006. Canopy CO_2 enrichment permits tracing the fate of recently assimilated carbon in a mature deciduous forest. New Phytol. 172, 319–329.

Klein, T., Hoch, G., 2015. Tree carbon allocation dynamics determined using carbon mass balance approach. New Phytol. 205, 147–159. http://dx.doi.org/10.1111/nph.12993.

Klein, T., Hoch, G., Yakir, D., Körner, C., 2014. Drought stress, growth and nonstructural carbohydrate dynamics of pine trees in a semi-arid forest. Tree Physiol. 34, 981–992. http://dx.doi.org/10.1093/treephys/tpu071.

Kozlowski, T.T., 1992. Carbohydrate sources and sinks in woody plants. Bot. Rev. 58, 107–222.

Kuptz, D., Fleischmann, F., Matyssek, R., Grams, T.E.E., 2011. Seasonal patterns of carbon allocation to respiratory pools in 60-yr-old deciduous (*Fagus sylvatica*) and evergreen (*Picea abies*) trees assessed via whole-tree stable carbon isotope labeling. New Phytol. 191, 160–172.

Lamlom, S.H., Savidge, R.A., 2003. A reassessment of carbon content in wood: variation within and between 41 North American species. Biomass Bioenergy 25, 381–388. http://dx.doi.org/10.1016/S0961-9534(03)00033-3.

Michelot, A., Eglin, T., Dufrêne, E., Lelarge-Trouverie, C., Damesin, C., 2011. Comparison of seasonal variations in water-use efficiency calculated from the carbon isotope composition of tree rings and flux data in a temperate forest. Plant Cell Environ. 34, 230–244. http://dx.doi.org/10.1111/j.1365-3040.2010.02238.x.

Palacio, S., Paterson, E., Sim, A., Hester, A.J., Millard, P., 2011. Browsing affects intra-ring carbon allocation in species with contrasting wood anatomy. Tree Physiol. 31, 150–159. http://dx.doi.org/10.1093/treephys/tpq110.

Pereira, J.S., Mateus, J.A., Aires, L.M., Pita, G., Pio, C., David, J.S., Andrade, V., Banza, J., David, T.S., Paço, T.A., Rodrigues, A., 2007. Net ecosystem carbon exchange in three contrasting Mediterranean ecosystems −the effect of drought. Biogeosciences 4, 791–802. http://dx.doi.org/10.5194/bg-4-791-2007.

R Core Team, 2014. R: A Language and Environment for Statistical Computing. R Foundation for Statistical Computing, Vienna, Austria, Vienna, Austria.

Ranson, K., Sun, G., Knox, R., Levine, E., Weishampel, J., Fifer, S., 2001. Northern forest ecosystem dynamics using coupled models and remote sensing. Remote Sens. Environ. 75, 291–302. http://dx.doi.org/10.1016/S0034-4257(00)00174-7.

Richardson, A.D., Hollinger, D.Y., Dail, D.B., Lee, J.T., Munger, J.W., O'keefe, J., 2009. Influence of spring phenology on seasonal and annual carbon balance in two contrasting New England forests. Tree Physiol. 29, 321–331. http://dx.doi.org/10.1093/treephys/tpn040.

Richardson, A.D., Williams, M., Hollinger, D.Y., Moore, D.J.P., Dail, D.B., Davidson, E.A., Scott, N.A., Evans, R.S., Hughes, H., Lee, J.T., Rodrigues, C., Savage, K., 2010. Estimating parameters of a forest ecosystem C model with measurements of stocks and fluxes as joint constraints. Oecologia 164, 25–40. http://dx.doi.org/10.1007/s00442-010-1628-y.

Richardson, A.D., Carbone, M.S., Keenan, T.F., Czimczik, C.I., Hollinger, D.Y., Murakami, P., Schaberg, P.G., Xu, X., 2013. Seasonal dynamics and age of stemwood nonstructural carbohydrates in temperate forest trees. New Phytol. 197, 850–861. http://dx.doi.org/10.1111/nph.12042.

Rocha, A.V., Goulden, M.L., Dunn, A.L., Wofsy, S.C., 2006. On linking interannual tree ring variability with observations of whole-forest CO_2 flux. Glob. Change Biol. 12, 1378–1389. http://dx.doi.org/10.1111/j.1365-2486.2006.01179.x.

Rossi, S., Deslauriers, A., Anfodillo, T., Morin, H., Saracino, A., Motta, R., Borghetti, M., Rossi, S., 2006. Conifers in cold environments synchronize maximum growth rate of tree-ring formation with day length. New Phytol. 170, 301–310.

Rossi, S., Deslauriers, A., Seo, J., Rathgeber, C.B.K., Anfodillo, T., Morin, H., Levanic, T., Oven, P., Jalkanen, R., 2008. Critical temperatures for xylogenesis in conifers of cold climates. Glob. Ecol. Biogeogr. 17, 696–707. http://dx.doi.org/10.1111/j.1466-8238.2008.00417.x.

Rustad, L.E., Fernandez, I.J., 1998. Experimental soil warming effects on CO_2 and CH_4 flux from a low elevation spruce-fir forest soil in Maine, USA. Glob. Change Biol. 4, 597–605. http://dx.doi.org/10.1046/j.1365-2486.1998.00169.x.

Skomarkova, M.V., Vaganov, E.A., Mund, M., Knohl, A., Linke, P., Boerner, A., Schulze, E.-D., 2006. Inter-annual and seasonal variability of radial growth, wood density and carbon isotope ratios in tree rings of beech (*Fagus sylvatica*) growing in Germany and Italy. Trees 20, 571–586. http://dx.doi.org/10.1007/s00468-006-0072-4.

Sun, G., Ranson, K.J., Guo, Z., Zhang, Z., Montesano, P., Kimes, D., 2011. Forest biomass mapping from lidar and radar synergies. Remote Sens. Environ. 115, 2906–2916. http://dx.doi.org/10.1016/j.rse.2011.03.021.

Thibeault-Martel, M., Krause, C., Morin, H., Rossi, S., 2008. Cambial activity and intra-annual xylem formation in roots and stems of *Abies balsamea* and *Picea mariana*. Ann. Bot. 102, 667–674. http://dx.doi.org/10.1093/aob/mcn146.

Thomas, C.K., Law, B.E., Irvine, J., Martin, J.G., Pettijohn, J.C., Davis, K.J., 2009. Seasonal hydrology explains interannual and seasonal variation in carbon and water exchange in a semiarid mature ponderosa pine forest in central Oregon. J. Geophys. Res. 114, 22. http://dx.doi.org/10.1029/2009JG001010.

Ueyama, M., Kai, A., Ichii, K., Hamotani, K., Kosugi, Y., Monji, N., 2011. The sensitivity of carbon sequestration to harvesting and climate conditions in a temperate cypress forest: observations and modeling. Ecol. Modell. 222, 3216–3225. http://dx.doi.org/10.1016/j.ecolmodel.2011.05.006.

Weishampel, J.F., Sung, G., Ransom, K.J., LeJeune, K.D., Shugart, H.H., 1994. Forest textural properties from simulated microwave backscatter: the influence of spatial resolution. Remote Sens. Environ. 47, 120–131. http://dx.doi.org/10.1016/0034-4257(94)90149-X.

Wharton, S., Falk, M., 2016. Climate indices strongly influence old-growth forest carbon exchange. Environ. Res. Lett. 11, 44016. http://dx.doi.org/10.1088/1748-9326/11/4/044016.

Wiley, E., Huepenbecker, S., Casper, B.B., Helliker, B.R., 2013. The effects of defoliation on carbon allocation: can carbon limitation reduce growth in favour of storage? Tree Physiol. 33, 1216–1228. http://dx.doi.org/10.1093/treephys/tpt093.

Young, H.E., Ribe, J.H., Wainwright, K., 1980. Weight Tables for Tree and Shrub Species in Maine. University of Maine, Orono, ME Misc. Rep. 230.

Zweifel, R., Eugster, W., Etzold, S., Dobbertin, M., Buchmann, N., Häsler, R., 2010. Link between continuous stem radius changes and net ecosystem productivity of a sub-alpine Norway spruce forest in the Swiss Alps. New Phytol. 187, 819–830. http://dx.doi.org/10.1111/j.1469-8137.2010.03301.x.